MGT: Supporting Information

Vanessa Meschke,[†] Andrew Novick,[†] Claire Porter,[†] Jennifer Rogers,[‡] Remco Chang,[‡] Thomas Proffen,[¶] and Eric S. Toberer*,[†]

†*Department of Physics, Golden, CO 80401*

‡*Department of Computer Science*

¶*Neutron Scattering Division*

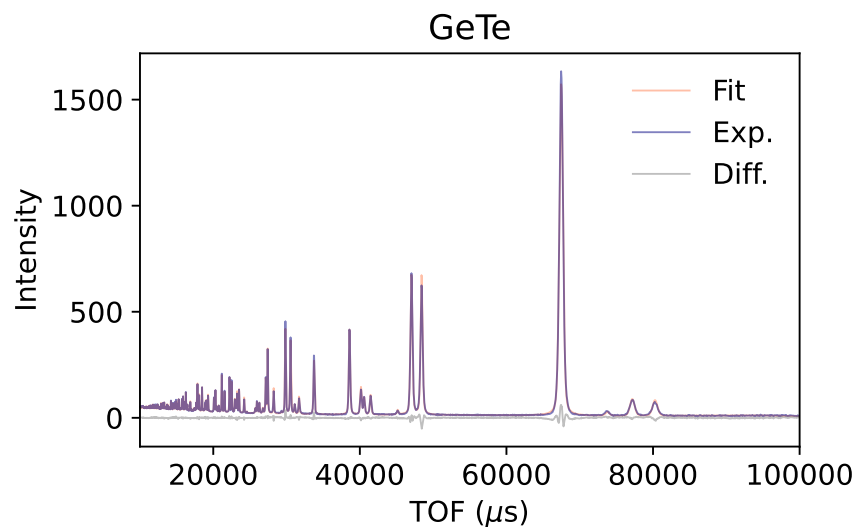E-mail: etoberer@mines.edu

1 Refined Time-of-Flight Patterns

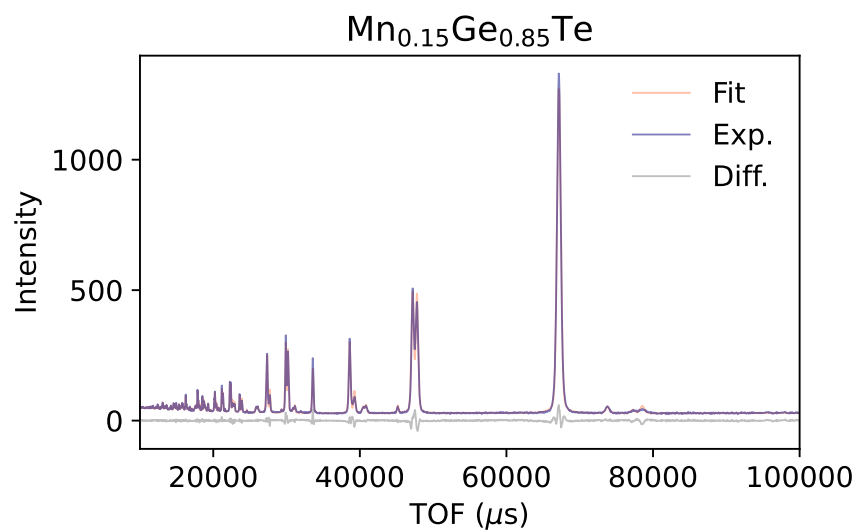Figure S1 Calculated time-of-flight pattern (orange) for GeTe. Sample had ~1% Ge impurity.

Figure S2 Calculated time-of-flight pattern (orange) for $Mn_{0.15}Ge_{0.85}Te$. Sample had ~1% Ge impurity.

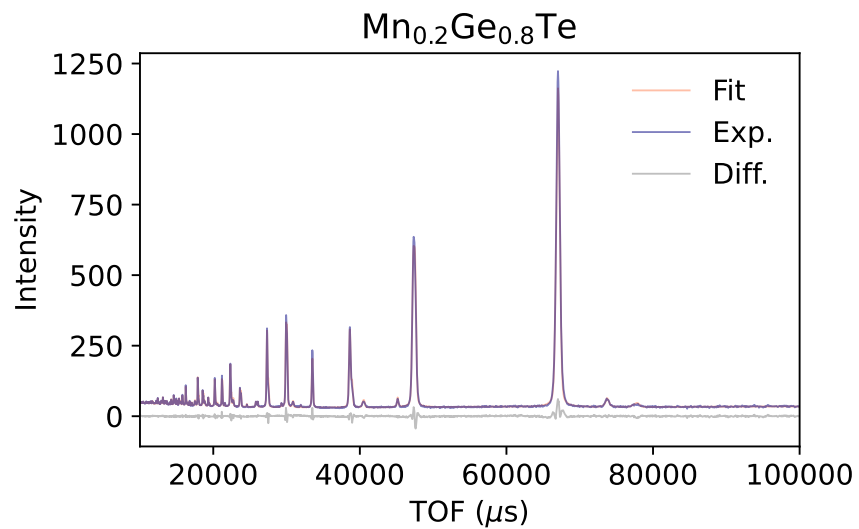Figure S3 Calculated time-of-flight pattern (orange) for $Mn_{0.2}Ge_{0.8}Te$. Sample had ~1% Ge impurity.

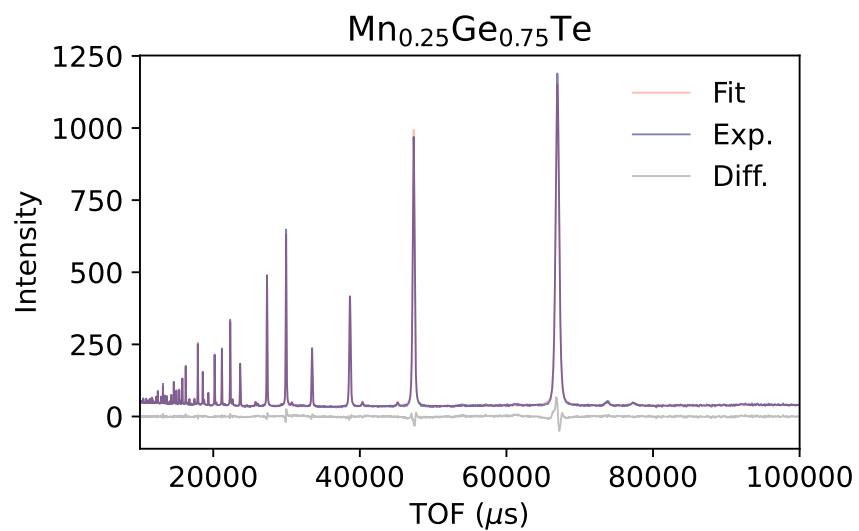Figure S4 Calculated time-of-flight pattern (orange) for $Mn_{0.25}Ge_{0.75}Te$. Sample had ~1% Ge impurity.
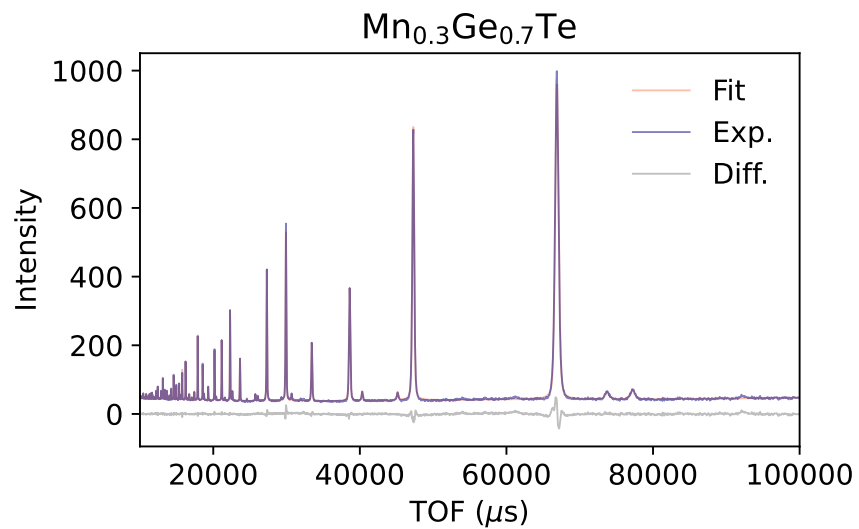
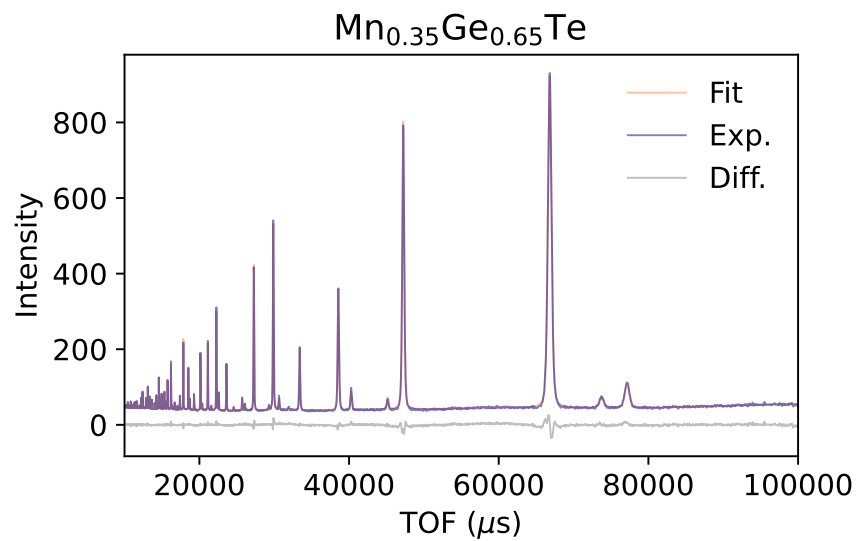Figure S5 Calculated time-of-flight pattern (orange) for $Mn_{0.3}Ge_{0.7}Te$. Sample had $\sim$1% Ge impurity.

Figure S6 Calculated time-of-flight pattern (orange) for $Mn_{0.35}Ge_{0.65}Te$. Sample had $\sim$1% Ge impurity.

2 Uncertainty Quantification

The uncertainty of each PDF at each point is calculated following the method outlined in Novick, et al, as $U = \sigma_{ens.,r}/\sqrt{n}$, where U is the uncertainty, $\sigma_{ens,r}$ is the standard deviation of the ensemble at point r, and n is the number of samples in the ensemble.
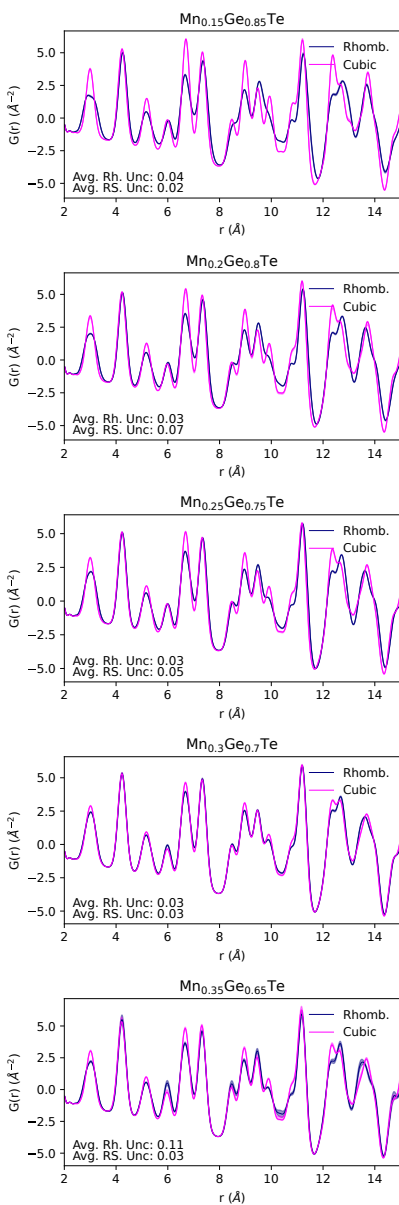

Figure S7 All uncertainties for the rhombohedral phase (navy) and the cubic phase (magenta).

3   Temperature Dependent Probability Distributions

Temperature dependent probability distributions ranging from 100K to 10 000K for all alloy compositions are shown below:
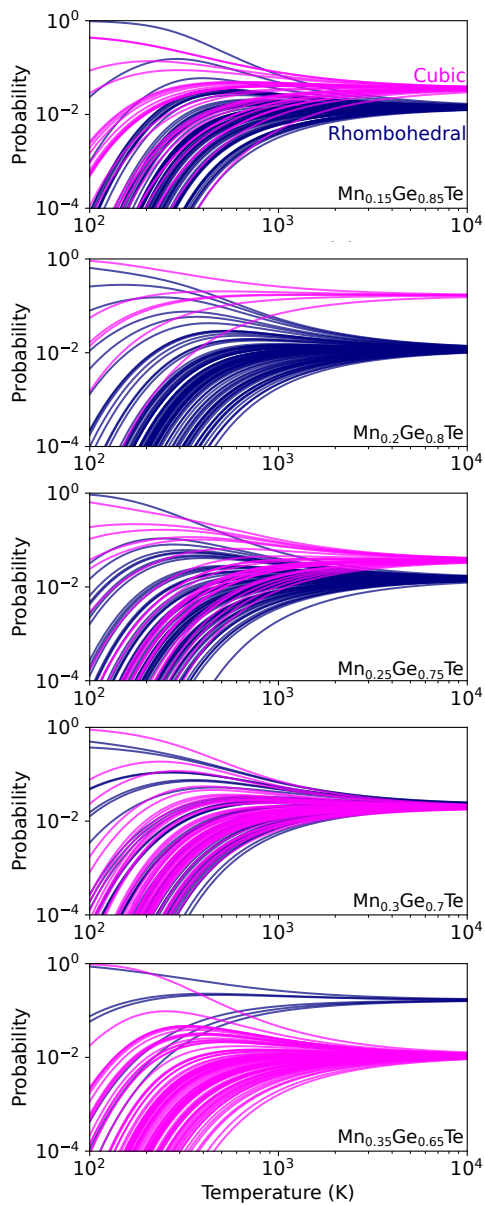

Figure S8 All temperature dependent probability distributions for the rhombohedral phase (navy) and the cubic phase (magenta).

4 Cation Averaged PDF Refinement

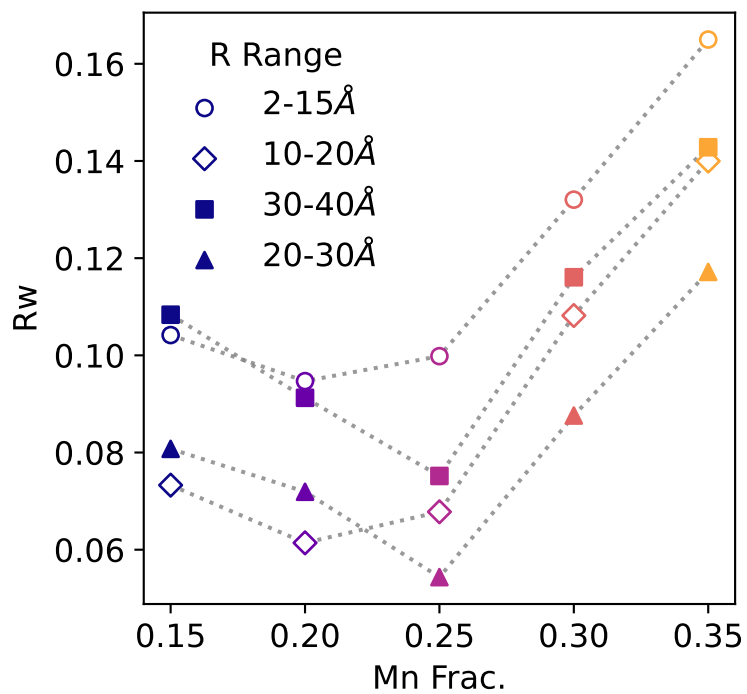The fit quality of the PDF refinements using the average structure approach are shown in Figure S9.

Figure S9 PDF refinements using the averaged structure approach for a variety of r ranges for all compositions.
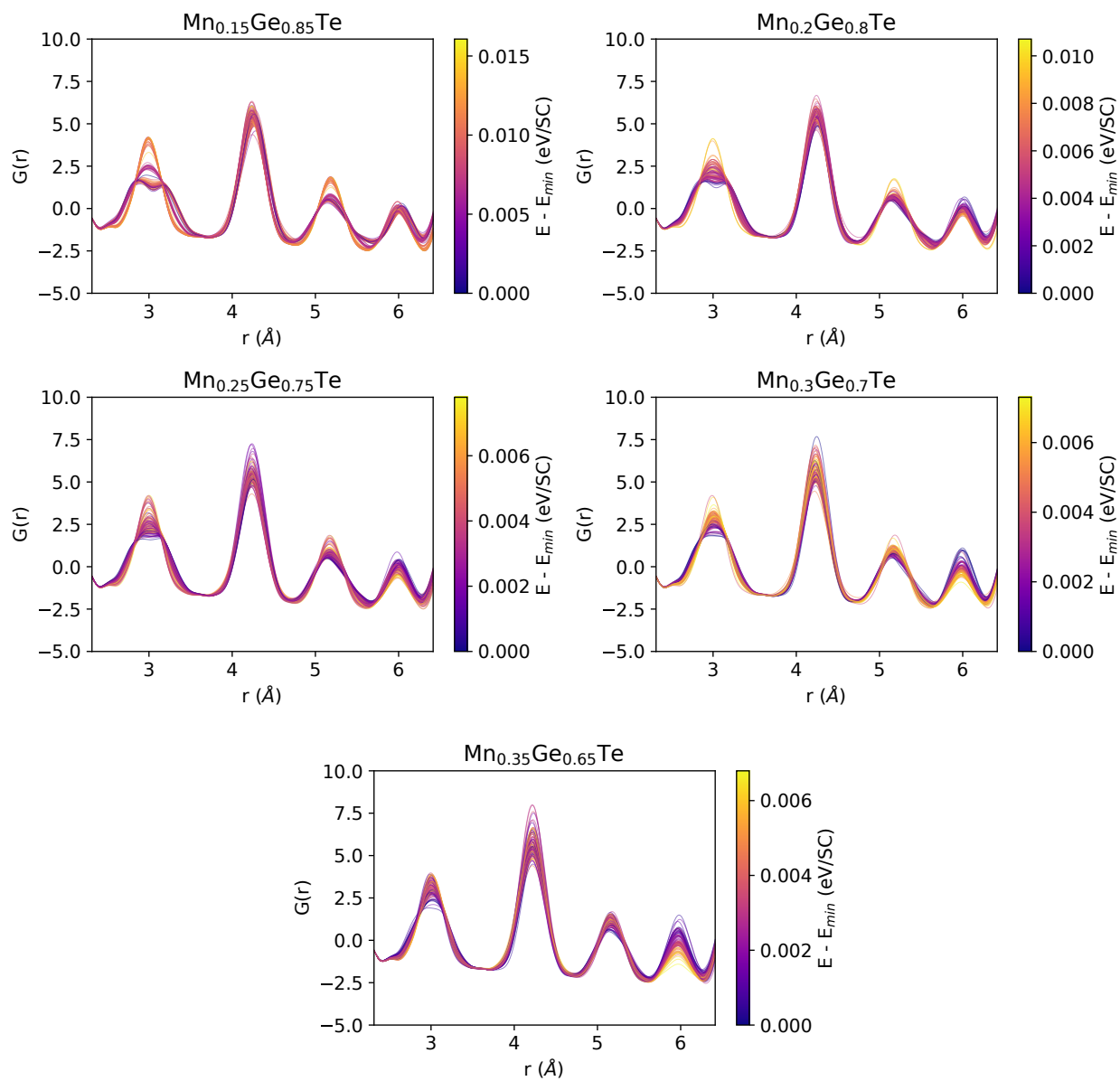
5 Individual PDFs

Figure S10 All PDFs for all supercells colored by supercell energy.

6 Individual Supercell Fit Quality

The fit quality for individually refined supercells as a function of energy is shown in Figure S11. Points shown are colored by composition. Additionally, supercells presenting as rhombohedral are shown as circles, while those presenting as rock salt are shown as squares. Structures were sorted based on characteristics of the first nearest neighbors peak in the PDF, as described in the main text. For the refinements, the lattice parameters were scaled isotropically to get a single lattice dilation constant used in the TEAPOT refinements. No distinct trend is apparent.
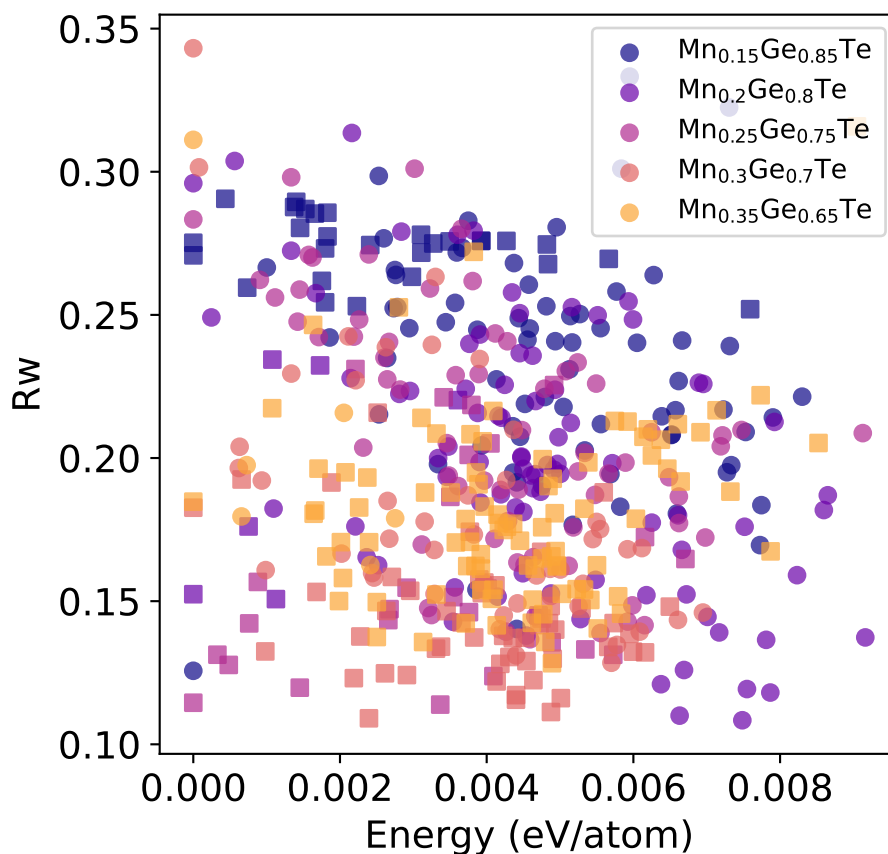

Figure S11 Rw for individual supercells as a function of energy. Points shown are coded by color (composition) and shape (square and circle for ending as rock salt and rhombohedral structures, respectively.)
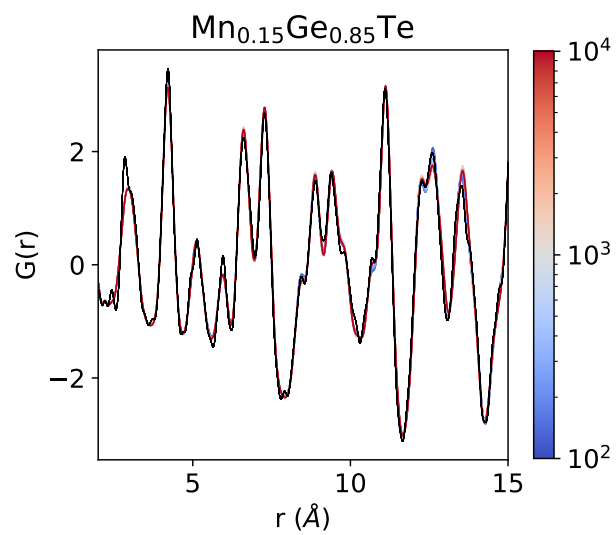
7 Temperature Dependent TEAPOT Fits

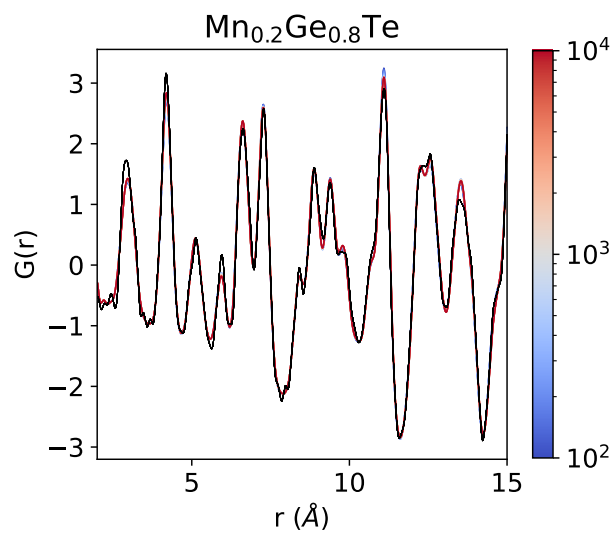Figure S12 TEAPOT PDF fits for every asserted temperature (color), with the experimental patterns shown in black.

Figure S13 TEAPOT PDF fits for every asserted temperature (color), with the experimental patterns shown in black.
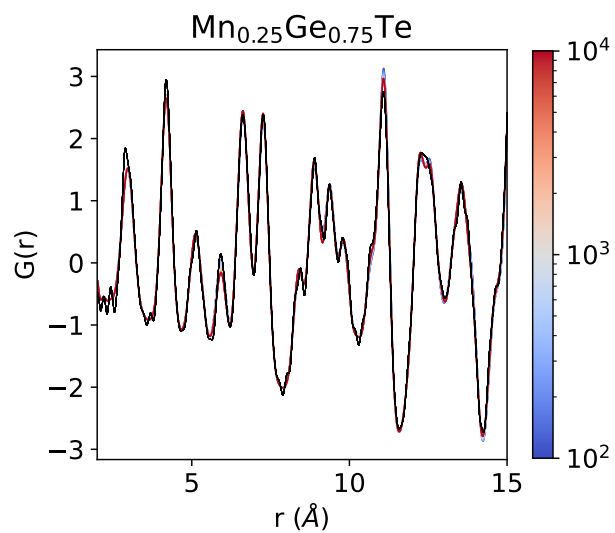

Figure S14 TEAPOT PDF fits for every asserted temperature (color), with the experimental patterns shown in black.
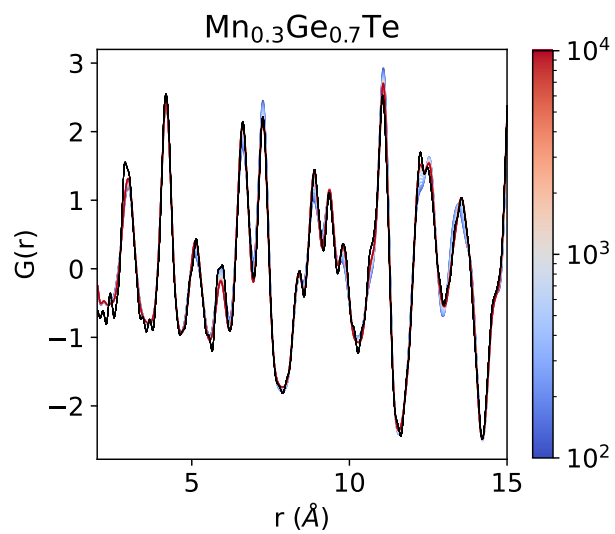
Figure S15 TEAPOT PDF fits for every asserted temperature (color), with the experimental patterns shown in black.
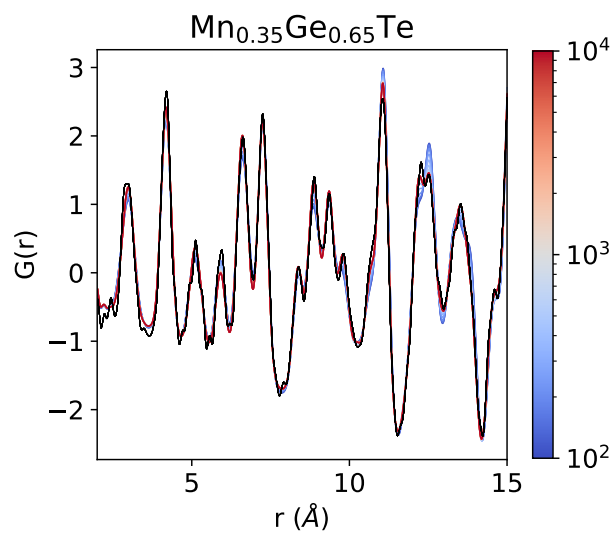

Figure S16 TEAPOT PDF fits for every asserted temperature (color), with the experimental patterns shown in black.
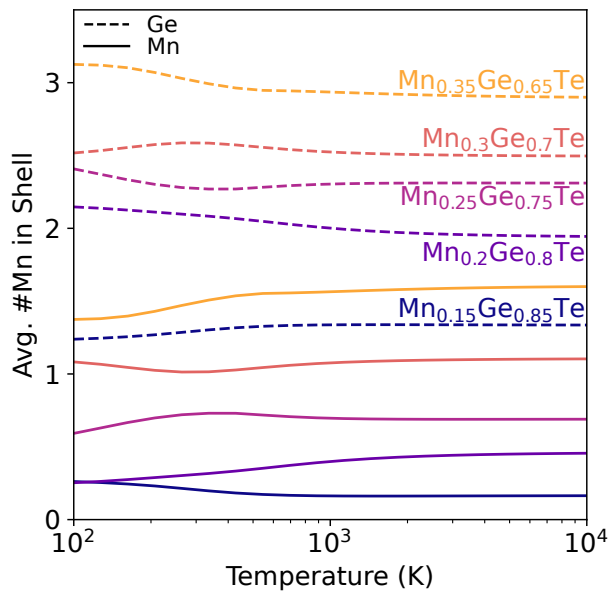
Figure S17 Average number of Mn in a second nearest neighbors coordination shell for each TEAPOT temperature probed.
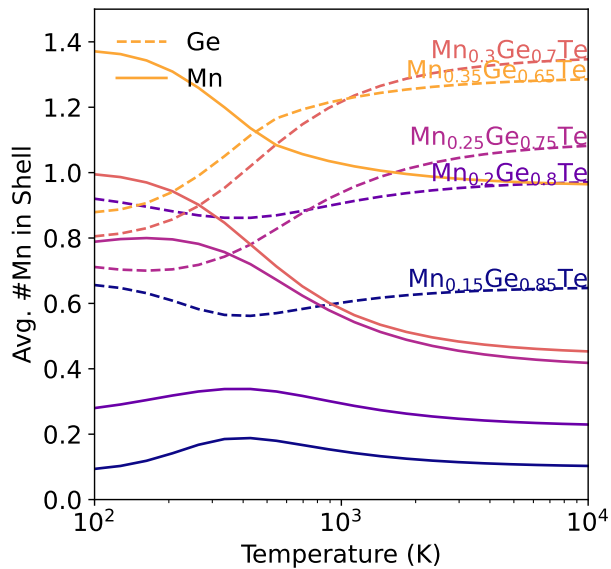

Figure S18 Average number of Mn in a fourth nearest neighbors coordination shell for each TEAPOT temperature probed.
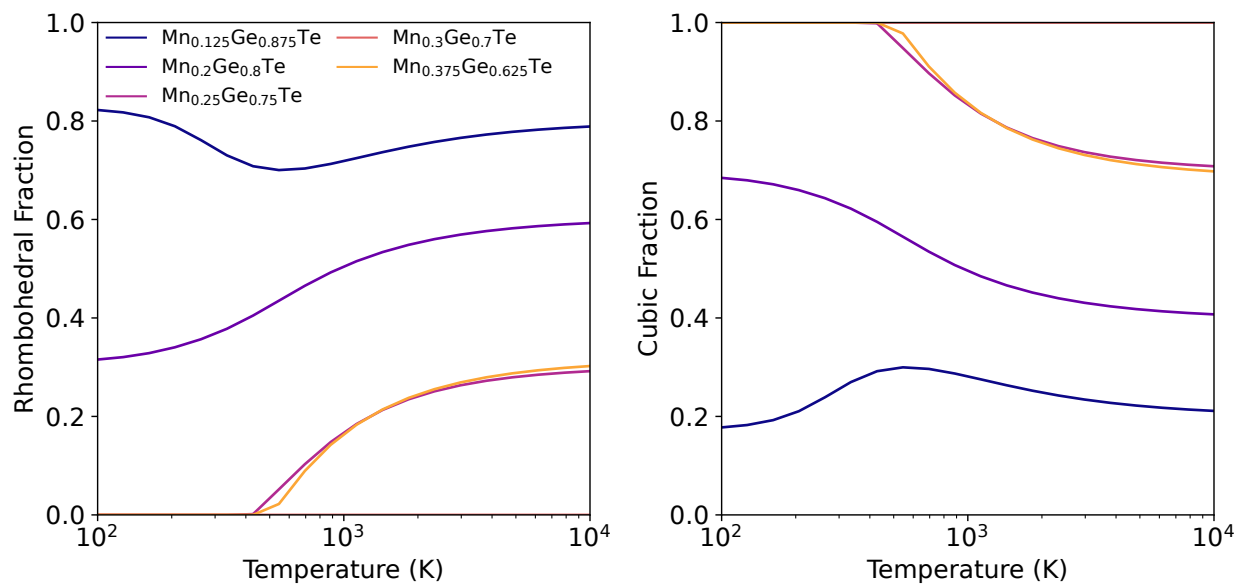
8 TEAPOT Fit Parameters vs. Temperature

Figure S19 Fractions of the rhombohedral (left) and cubic (right) ensembles that were present at the end of the TEAPOT refinement at each calculation temperature.
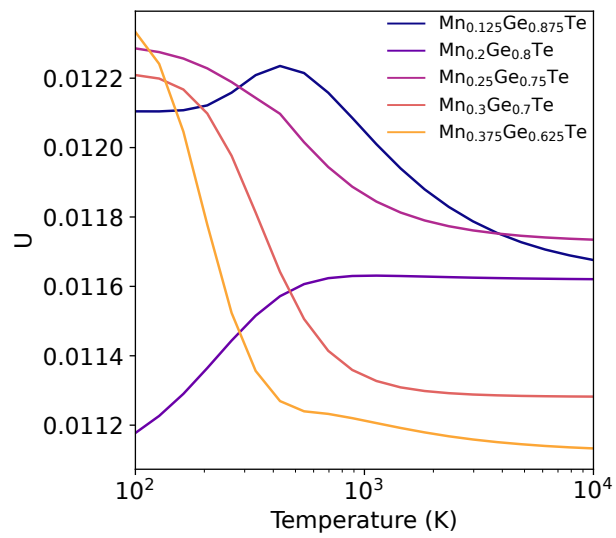
Figure S20 The atomic displacement parameters at the fitting for each temperature in the ensemble refinement.